IEEE Access
Multidisciplinary | Rapid Review | Open Access Journal

Received 5 March 2024, accepted 8 April 2024, date of publication 17 April 2024, date of current version 26 April 2024.

Digital Object Identifier 10.1109/ACCESS.2024.3390154

RESEARCH ARTICLE

H_∞ Control for Energy Dispatch in Autonomous Nanogrid With Communication Delays

YOUNGWOO LEE[1], (Member, IEEE), YONGHAO GUI[2], (Senior Member, IEEE), AND WONHEE KIM[3], (Member, IEEE)

[1]Division of Electrical Engineering, Hanyang University, ERICA Campus, Ansan 15588, South Korea
[2]Electrification and Energy Infrastructures Division, Oak Ridge National Laboratory, Knoxville, TN 37932, USA
[3]School of Energy Systems Engineering, Chung-Ang University, Seoul 06974, South Korea

Corresponding author: Wonhee Kim (whkim79@cau.ac.kr)

This work was supported in part by the Institute of Information and Communications Technology Planning and Evaluation (IITP) Grant funded by the Korean Government through the Ministry of Science and ICT (MSIT) (Artificial Intelligence Innovation Hub) under Grant 2021-0-02068; in part by the Climate Change Response Technology Development Program through NFR by MSIT under Grant NRF-2021M1A2A2065445; in part by the Ministry of Trade, Industry and Energy (South Korea) under Project titled by "The Development of 22 kW Class High Power Density LDC Integrated Bidirectional Vehicle Charger;" and in part by the NRF Grant funded by the Korean Government through MSIT under Grant 2022R1F1A1075479.

ABSTRACT This paper proposes an optimal controller and estimator for energy dispatch to balance the power supply and demand considering communication delays. The proposed algorithm involves modeling an autonomous nanogrid (ANG) consisting of distributed energy resources, energy storage systems, loads, an H_∞ controller with a reference power modulation technique, and a state estimator. The ANG was developed to express the dynamic supply-demand energy balance of a nanogird system. Reference power modulation was designed to generate the desired ESS power based on the imbalanced energy. Random communication delays were modeled using a stochastic variable satisfying the Bernoulli random binary distribution. The optimal H_∞ controller and estimator were developed using a linear matrix inequality approach to exponentially stabilize the closed-loop system. Simulations were performed using real daily demand forecasts obtained from the Korea Meteorological Administration to demonstrate the effectiveness of the proposed real-time optimization algorithm.

INDEX TERMS Autonomous nanogrid system, energy dispatch, communication delay, H_∞ control, energy storage system, distributed energy resource.

I. INTRODUCTION

Over the past few decades, incorporating small distributed energy resources (DERs), such as photovoltaics (PVs), wind turbines, and fuel cells into microgrid (MG) systems has become necessary because of the growing demand for a self-sufficient electricity supply. In particular, MGs provide a promising solution for DERs, energy storage system (ESSs), and connected loads in power distributed networks [1], [2]. However, there is an urgent need for power coordination between supply and demand to achieve a reliable supply-demand energy balance from economic dispatch [3] because of the intermittent characteristics of DERs and short-term load demand variations.

Recently, a new concept called a "nanogrid (NG)", which is a smaller version of an MG for even greater efficiency and flexibility has been proposed [4], [5], [6]. An NG is a decentralized and small-scale power grid that provides electricity to isolated communities and remote areas. The components of NGs typically include DERs, ESSs, power electronics, and power management systems as well as various residential loads, such as TVs, electric ovens, washing machines, heating/air conditioning systems, and refrigerators in households and commercial buildings [7], [8], [9]. Generally, there are two modes of NG: grid-connected and stand-alone. In particular, it is more important to guarantee the stability of stand-alone NGs than that of

The associate editor coordinating the review of this manuscript and approving it for publication was Youngjin Kim.

grid-connected NG because it is impossible to supply load demand power from grid-connected utility. As stand-alone NGs are not connected to a larger grid, they rely on local power resources to satisfy the power load demands. Therefore, several energy dispatch approaches have been developed to address this problem in MGs and NGs [3], [10], [11].

However, two main issues must be considered to achieve a reliable supply-demand energy balance. First, it is impossible to forecast the daily demand because there are several interactive demands that can be turned on or off as per consumer needs such as TVs, microwaves, and air conditioners in households and buildings. To address this problem, real-time optimization is necessary to supply power corresponding to high instantaneous load demands. When implementing a real-time optimization algorithm for energy dispatch, all the components are connected to an NG central controller and energy exchange can occur in both directions between the ESSs, DERs, and loads in the NG networks. In this respect, various forecasting approaches have been proposed to compensate for significant uncertainties [12], [13], [14]. However, it is not easy to reduce forecasting error because of the high instantaneous demands. Second, the network itself is a dynamic system that induces possible delays in network communication owing to its limited bandwidth. A realistic network control system design should consider communication delays because these delays are widely known to degrade the system performance [15]. Especially, misinformation owing to communication delays can cause critical energy imbalance problems and blackouts in real-time implementation. Therefore, a real-time optimization algorithm should be developed to compensate for the effects of communication delays. Random communication delays have been researched to ensure robust performance in various networked systems [16], [17], [18]. However, the communication delay problem can cause serious performance degradation in systems that must guarantee real-time control performance, such as NGs. There has been no study on the communication delay problem in nanogrid.

In this paper, we propose an H_∞ controller for energy dispatch to compensate for the effects of communication delays. An autonomous NG (ANG) system was developed to express the dynamic supply-demand energy balance of an NG system. Herein, the dynamics and constraints of the load demand, ESSs, and DERs were modeled. Reference power modulation was designed for the desired ESS power generation based on the imbalanced energy. Consequently, the communication delays between the digital processor and the physical system were modeled using independent Bernoulli random variables. Based on the mathematical models, an H_∞ controller and estimator were developed to compensate for the communication delays. To implement the proposed ANG system network, a linear matrix inequality (LMI) condition was developed to satisfy the H_∞ control performance and stability for given communication delays. Finally, simulations were performed to demonstrate the effectiveness of the proposed real-time optimization algorithm. For realistic simulations, the load demand forecast and DER power were generated based on experimental data from the Korea Meteorological Administration. The main contributions of this paper are summarized as follows:

- An ANG system was modeled for reliable dynamic supply-demand energy balance.
- Communication delays were considered to implement a realistic NG network system.
- The controller and estimator were designed to compensate for communication delays.

The remainder of this paper is organized as follows: Section II introduces system modeling with the constraints of an NG. The reference power modulation, controller, and estimator considering communication delays are described in Section III. The stability and H_∞ performance are described in Section IV. The simulation results are presented in Section V. Finally, Section VI concludes the paper.

II. SYSTEM MODELING

In this section, we describe the constraints of NG components and the model of an ANG system.

A. DYNAMICS AND CONSTRAINTS OF AN NG SYSTEM

1) LOAD DEMAND

In general, two types of loads exist: interactive and background. The interactive loads are home appliances that consumers can turn on or off as required, such as TVs, microwaves, washing machines, and air conditioners. The background loads are home appliances that must be constantly turned on, such as refrigerators. In NG systems, as humans have different daily life style, it is impossible to predict the total load demand. Therefore, the total NG demand at time k is denoted as follows:

$$\begin{aligned} P_k^L &= P_k^{B.L} + \Delta P_k^L \\ P^{L.min} &\le P_k^L \le P^{L.max} \\ \Delta P^{L.min} &\le \Delta P_k^L \le \Delta P^{L.max} \end{aligned} \tag{1}$$

where P_k^L denotes the total demand, $P_k^{B.L}$ and ΔP_k^L denote the interactive demand and background demand, respectively. $P^{L.min}$ and $P^{L.max}$ denote the minimum and maximum total demands, respectively. $\Delta P^{L.min}$ and $\Delta P^{L.max}$ are the minimum and maximum interactive demands, respectively. For the default load case, $\Delta P^{L.min}$ is considered zero.

2) ESS

ESSs (such as battery and supercapacitor) are important for satisfying the energy balance between the load demand and supply in NGs. Especially, they allow a smooth intermittent RES power flow and provides peak power load shaving. For ESSs, as the charging and discharging capacities are bounded, the following inequality constraints are reasonable:

$$\begin{aligned} 0 &\le E_k^{ch} \le E^{ch.max} \\ E^{dch.min} &\le E_k^{dch} \le 0 \end{aligned} \tag{2}$$

where E_k^{ch} and E_k^{dch} denote the charging and discharging powers at time k, respectively. $E^{ch.max}$ and $E^{dch.min}$ denote

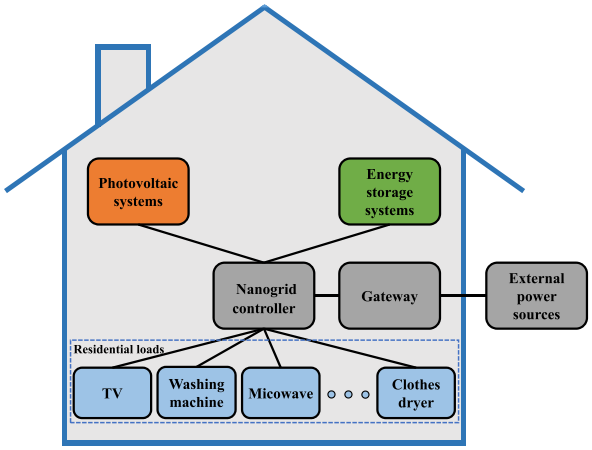

FIGURE 1. Architecture of a typical nanogrid system.

the maximum charging limit and minimum discharging limit, respectively. The life time of an ESS depends critically on its repeated charging and discharging efficiencies. Therefore, the ESS dynamics can be represented by the conversion efficiencies of the charging/discharging efficiency as follows:

$$E_{k+1} = E_k + (1 - S_k)\eta^{ch} E_k^{ch} + S_k \frac{1}{\eta^{dch}} E_k^{dch} \tag{3}$$

where S_k denotes the ESS switching function. Here, $S_k = 1$ refers to the discharge mode of the ESS. By contrast, S_k should be zero in the ESS charging mode.

3) DER

Various types of DERs, such as PV generators, are uncontrollable and their output power depends on the utilization of natural sources. In such cases, the following constraint for the DER holds:

$$P^{DER.min} \leq P_k^{DER} \leq P^{DER.max} \tag{4}$$

where P_k^{DER} denotes the total DER generation capacity. $P^{DER.min}$ and $P^{DER.max}$ denote the minimum output power and maximum output power generated by the DER, respectively.

B. ANG SYSTEM

At each time interval, the energy balance equation can be formulated using (1) (2), and (4) as follows:

$$P_k^{B.L} + \Delta P_k^L + E_k^{ch} = P_k^{DER} + E_k^{dch} \tag{5}$$

The ANG state space model can then be expressed using (3) as follows:

$$\begin{aligned} x_{k+1} &= \Phi x_k + \Gamma u_k \\ y_k &= C x_k \end{aligned} \tag{6}$$

where $x_k = \left[E_k\right]$, $u_k = \left[E_k^{ch}\ E_k^{dch}\right]^T$, $y_k = x_k$, $\Phi = \left[1\right]$, $\Gamma = \left[(1 - S_k)\eta^{ch}\ \frac{S_k}{\eta^{ch}}\right]^T$, $C = \left[1\right]$. Here, the matrices Φ, Γ, and C denote the state, input, and output matrices, respectively. The architecture of a typical NG consisting of a DER, an ESS, a residential load, and a gateway is shown in Fig. 1. However, an optimal controller corresponding to the energy imbalance is necessary because the charging input power and discharging input power of the ESS should be controlled to balance the energy supply and demand. This will be discussed in the following section.

III. REFERENCE POWER MODULATION AND COMMUNICATION DELAY

In this section, the design problem of the ESS reference power is addressed to achieve an energy balance. Subsequently, the ANG model is reformulated to address the practical problems caused by communication delays.

A. REFERENCE POWER MODULATION

To address the energy imbalance problem, the state of an ESS needs to be identified. The ESS energy status needs to be updated using the information of the state of charge (SOC). Therefore, we propose the following reference power modulation for the desired ESS power generation:

$$x_j^d = E_j - \Delta E_j^{ch/dch}, \quad (\because j = nk) \tag{7}$$

where j denotes the sample time index in the reference update and n is a positive integer. $\Delta E_j^{ch/dch} = P_j^L - P_j^{DER}$. Recall the ANG system of (6), because the ANG system can be reformulated to handle the communication delay problem, the generalized ANG system of (6) can be represented as follows:

$$\begin{aligned} x_{k+1} &= \Phi x_k + \Gamma u_k + \Gamma_w w_k \\ z_k &= D x_k + F_u u_k + F_w w_k \\ y_k &= C x_k + C_w w_k \end{aligned} \tag{8}$$

where w_k denotes the exogenous disturbance signal vector, Γ_w, C_w, D, F_u, and F_w denote the designer's choice variables and belong to the set of square summable sequences $\ell_2[0, \infty)$. The following assumptions are used in the optimization-based controller design [19]:

Assumption 1:

1) (Φ, Γ) is stabilizable;
2) $F_u^T F_u$ is invertible;
3) $F_u^T D = 0$;
4) (D, Φ) has no unobservable modes on the imaginary axis.

$\Diamond$

B. ANG SYSTEM WITH COMMUNICATION DELAY

In this subsection, the input communication delay and output communication delay can be described for the generalized ANG system (8) as follows:

$$\begin{aligned} y_{cd.k} &= (1 - \alpha) y_k + \alpha y_{k-1}, \\ u_{cd.k} &= (1 - \beta) u_k + \beta u_{k-1}, \end{aligned} \tag{9}$$

where α and β are the input Bernoulli random variables and the output Bernoulli random variables, respectively. Consequently, these delays have the following distributions:

$$\begin{aligned} \mathbb{P}\{\alpha = 1\} &= \bar{\alpha} \in [0, 1], \\ \mathbb{P}\{\beta = 1\} &= \bar{\beta} \in [0, 1], \end{aligned} \tag{10}$$

$\alpha = 1$ indicates that there is a one-step delay from the measurement to the controller. If $\beta = 1$, the one-step delay is modeled from the controller to the generalized ANG. Using (9) and (11), the controller and estimator can be developed as follows:

$$\begin{aligned} \textit{Controller}: & \quad u_k = -K(x_k^d - \hat{x}_k) \\ & \quad u_{cd.k} = (1-\beta)u_k + \beta u_{k-1} \\ \textit{Estimator}: & \quad \hat{x}_{k+1} = \Phi\hat{x}_k + \Gamma u_{cd.k} + L(y_{cd.k} - \bar{y}_{cd.k}) \\ & \quad \bar{y}_{cd.k} = (1-\bar{\alpha})C\hat{x}_k + \bar{\alpha}C\hat{x}_{k-1} \end{aligned} \tag{11}$$

where $\hat{x}_k$ denotes the estimated state variable. $\bar{y}_{cd.k}$ denotes the estimated output considering the communication delays. K and L denote the controller and observer gains, respectively. The stochastic variable β, which is mutually independent of α, is also a Bernoulli distributed white sequence with the expected value $\bar{\beta}$. For a simple formulation, we assume that the ESS has no surplus power when satisfying a reliable supply-demand energy balance, that is $x_k^d = 0$.

Remark 1: The output y_k produced at time k is sent to the observer via a communication channel and arrives at time $k+\tau_d$. If the sampling period is long compared with τ_d, there is no need to consider the influence of the delay. If τ_d is longer than unit sampling period and shorter than over two sampling periods, then the output $y_{cd.k} = y_{k-1}$. It can be observed that, at the k^{th} sampling time, the actual system output takes the value y_{k-1} with probability $\bar{\alpha}$, and the value y_{k-1} with probability $1-\bar{\alpha}$. If the binary stochastic variable $\bar{\alpha}$ takes the value 1 consecutively at different sample times, long time delays would occur. ◊

The corresponding robust control problem with random communication delays will become more important, and the results will appear in the near future. The estimation error is defined as follows:

$$e_k = x_k - \hat{x}_k. \tag{12}$$

By substituting (9) and (11) into (8) and (12), respectively, we obtain the closed-loop system as follows:

$$\chi_{k+1} = (\bar{\Phi} + \tilde{\Phi})\chi_k - \bar{\Gamma}w_k, \tag{13}$$

where χ, $\bar{\Phi}(y_k)$, and $\bar{\Gamma}$ can be found in (14). To verify the stability of the closed-loop system in (13), let us introduce the following definitions:

$$\begin{aligned} \chi_k &= \begin{bmatrix} x_k & e_k & x_{k-1} & e_{k-1} \end{bmatrix}^T \\ \bar{\Phi} &= \begin{bmatrix} \Phi+\psi_1 & -\psi_1 & \psi_2 & -\psi_2 \\ 0 & \Phi-\psi_3 & 0 & -\psi_4 \\ I & 0 & 0 & 0 \\ 0 & I & 0 & 0 \end{bmatrix} \\ \psi_1 &= (1-\bar{\beta})\Gamma K, \ \psi_2 = \bar{\beta}\Gamma K \\ \psi_3 &= (1-\bar{\alpha})LC_1, \ \psi_2 = \bar{\alpha}LC_1 \\ \tilde{\Phi} &= \begin{bmatrix} -\Delta_1 & \Delta_1 & \Delta_1 & -\Delta_1 \\ \Delta_2 & 0 & -\Delta_2 & 0 \\ 0 & 0 & 0 & 0 \\ 0 & I & 0 & 0 \end{bmatrix} \end{aligned}$$

$$\begin{aligned} \Delta_1 &= (\beta - \bar{\beta})\Gamma K, \ \Delta_2 = (\alpha - \bar{\alpha})LC_1 \\ \bar{\Gamma} &= \begin{bmatrix} \Gamma_w & (1-\alpha)LC_w\Gamma_w & 0 & 0 \end{bmatrix}^T \end{aligned} \tag{14}$$

Definition 1: The origin of the closed-loop system (13) is exponentially stable with $w_k = 0$, if there exists positive constant q and $\tau \in (0,1)$ such that for all non-negative constant k,

$$\mathbb{E}\{||\chi_k||^2\} \le q\tau\mathbb{E}\{||\chi_0||^2\}, \ \chi_0 \in \mathbb{R}^n. \tag{15}$$

◊

Therefore, the H_∞ performance of the controlled output z can be expressed by the following definition.

Definition 2: For a given positive γ with a zero-initial condition, the controlled output z satisfies the H_∞ performance if under a non-zero condition w_k for all k, z satisfies the following inequality:

$$\sum_{k=0}^{\infty}\mathbb{E}\{||\chi_k||\}^2 < \gamma^2\sum_{k=0}^{\infty}\mathbb{E}\{||\chi_0||\}^2. \tag{16}$$

◊

From Definitions 1 and 2, exponential stability and H_∞ performance can be guaranteed for the closed-loop system (13) in spite of the communication delays.

IV. CLOSED-LOOP STABILITY AND H_∞ OPTIMAL PERFORMANCE

In this section, we solve the closed-loop stability and H_∞ performance problem in (13) by using the Lyapunov theorem.

A. CLOSED-LOOP STABILITY

First, a matrix inequality condition can be derived to demonstrate the exponential stability of the closed-loop system by introducing the following lemma:

Lemma 1: Consider a Lyapunov candidate function $V(\chi_k)$. Suppose that there exists real numbers $\lambda \ge 0$, $\mu_{min} > 0$, $\mu_{max} > 0$, and $0 < \varphi < 1$ such that

$$\begin{aligned} &\mu_{min}||\chi_k||^2 \le V(\chi_k) \le \mu_{max}||\chi_k||^2, \\ &\mathbb{E}\{V(\chi_{k+1})|\chi_k\} - V(\chi_k) \le \lambda - \varphi V(\chi_k) \end{aligned} \tag{17}$$

so that the sequence χ_k satisfies

$$\mathbb{E}\{||\chi_k||^2\} \le \frac{\mu_{max}}{\mu_{min}}||\chi_0||^2(1-\varphi)^k + \frac{\lambda}{\mu_{min}\varphi}. \tag{18}$$

◊

Proof 1: This proof can be similarly refered in [15]. ■

By considering Theorem 1, we can confirm that the origin of the closed-loop system is exponentially stable when the corresponding matrix inequality is satisfied in the following Theorem 1.

Theorem 1: By applying the controller gain K and estimator gain L, the closed-loop system (13) with $w_k = 0$ guarantee exponentially stability if there exist positive-definite matrices P_1, S_1, P_2 and S_2 satisfying the matrix inequality in (28) with $\kappa_1 = \sqrt{(1-\bar{\alpha})\bar{\alpha}}$, $\kappa_2 = \sqrt{(1-\bar{\beta})\bar{\beta}}$. ◊

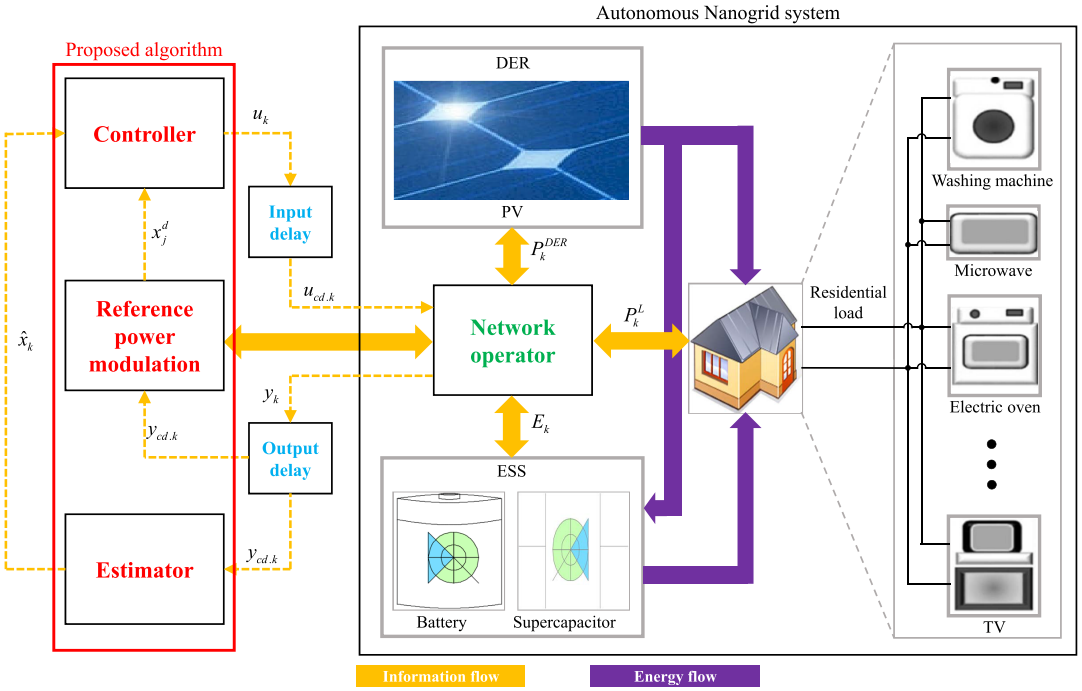

FIGURE 2. Block diagram with the proposed algorithm in an autonomous nanogrid system.

B. H_∞ CONTROLLER DESIGN

In this subsection, the H_∞ controller is developed to handle the robust problem for the H_∞ performance given in Definition 2. We obtained the following result:

Theorem 2: Consider a given positive γ. Suppose that there exist positive-definite matrices P_1, S_1, P_2, and S_2, and real matrices K and L satisfying the matrix inequality in (31), as shown subsequently. Then, the closed-loop system (13) is exponentially stable and satisfies the H_∞ performance with the controlled output z. ◊

Because (28) is not an LMI form, this equation is converted into an LMI form. For full-column rank Γ, we can assume that matrices U and V are orthogonal matrices of Γ as follows:

$$U\Gamma V = \begin{bmatrix} U_1 \\ U_2 \end{bmatrix} \Gamma V = \begin{bmatrix} \Sigma \\ 0 \end{bmatrix}, \tag{19}$$

where Σ is a nonsingular diagonal matrix. Σ consists of non-zero singular values of Γ. Thus, we have the following theorem and the proof is similar to that of Theorem 2 (cited in [15]).

Theorem 3: Consider the closed-loop system (13) with a given positive γ. The origin of the closed-loop system (13) is exponentially stable and also guarantee the H_∞ performance with the controlled output z when

- A positive-definite matrix P_1 exists with P_{11} and P_{12}, where

$$P_1 = U^T \begin{bmatrix} P_{11} & 0 \\ 0 & P_{12} \end{bmatrix} U, \; P_{11} > 0, \; P_{12} > 0, \tag{20}$$

  with U_1 and U_2 given in (19);
- Positive definite matrices S_1, S_2, and P_2 exist;
- Real matrices M and N exist,

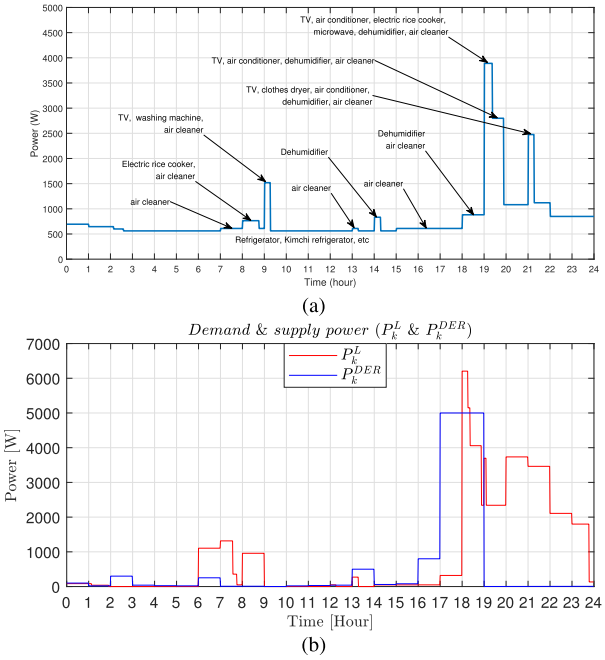

FIGURE 3. Demand and supply power: (a) type of home appliances and its power consumption, (b) total forecasted demand power and DER power.

such that the LMI in (32) is satisfied. Furthermore, the corresponding H_∞ controller can be obtained by

$$\begin{aligned} K &= V\Sigma^{-1}P_{11}^{-1}\Sigma V^T M \\ L &= S_1^{-1}N. \end{aligned} \tag{21}$$

◊

It is important to discuss the H_∞ performance against communication delays according to the smallest value of γ.

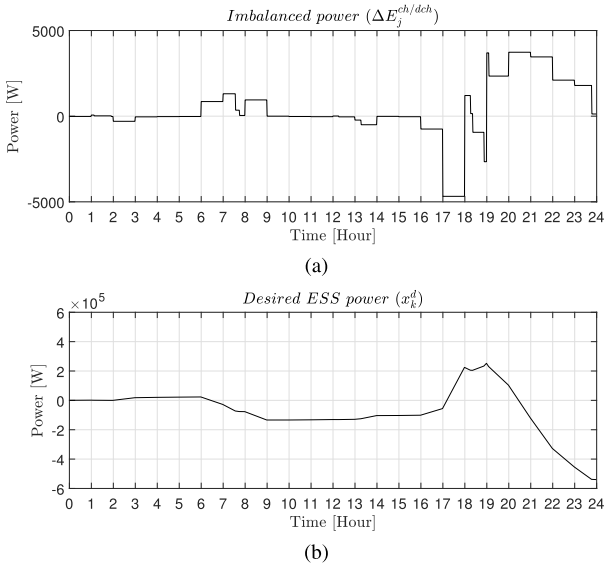

FIGURE 4. Imbalanced power and desired ESS power: (a) imbalanced power, (b) desired ESS power.

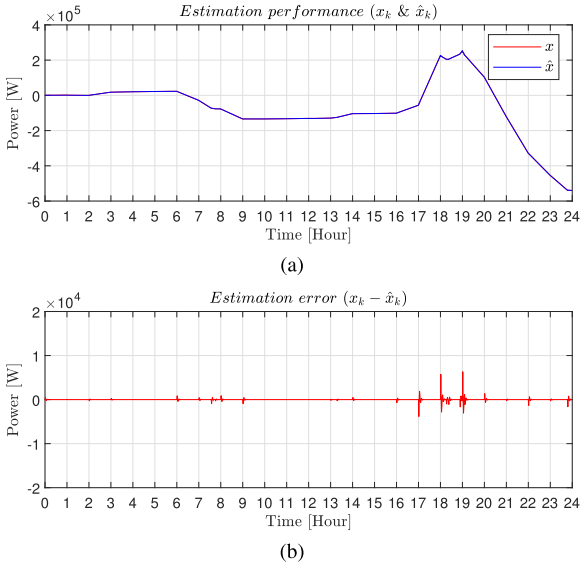

FIGURE 5. Estimation performance and estimation error: (a) estimation performance, (b) estimation error.

Note that γ can be decided as arbitrarily large to satisfy the H_∞ performance in the H_∞ controller (21). Then the optimal H_∞ performance can be guaranteed by solving the following convex optimization problem:

$$\begin{aligned} &min\ \gamma \\ &subject\ to\ (32) \\ &P_1,\ S_1,\ P_1, and\ S_1 > 0,\ M,\ N. \end{aligned} \tag{22}$$

Using the γ from (22), we can characterize the H_∞ controller using (21) in (8). Notice that, the H_∞ controller can ensure exponential stability and also guarantee the optimal H_∞ performance with communication delays in the closed-loop system (8). A block diagram of the proposed total energy management controller in an ANG system with communication delays is shown in Fig. 2.

V. SIMULATION RESULTS

In this section, we demonstrate the effectiveness and applicability of the proposed method using MATLAB/Simulink. For a realistic simulation, the total forecast demand and DER power were determined by referring to the Korea Electric Power Exchange and Korea Meteorological Administration [20], [21].

A. SIMULATION SETUP

The total daily demand forecast is obtained from the sum of the daily demand forecasts for each appliance, as shown in Fig. 3(a). The PV power data for August 28, 2022, based on a facility capacity of 3 kW, were obtained from the Korea Meteorological Administration. The PV power and forecast demand data are provided in hours and minutes, respectively. To demonstrate the effectiveness of the proposed controller in the presence of communication delays, we performed simulations for the following four cases as follows:

- Case 1: Classical control without communication delays,
- Case 2: Classical control with communication delays,
- Case 3: Proposed control with communication delays,
- Case 4: Predictor with communication delays [22], [23], [24].

The predictor has been widely applied to identify delays; therefore it is used to compare tracking performance as a classical delay estimator as follows:

$$\begin{aligned} \hat{y}_k &= y_{cd.k-1} + \left(\frac{y_{cd.k-1} - y_{cd.k-2}}{T_s}\alpha\right), \\ \hat{u}_k &= u_{cd.k-1} + \left(\frac{u_{cd.k-1} - u_{cd.k-2}}{T_s}\beta\right), \end{aligned} \tag{23}$$

where $\hat{y}_k$ and $\hat{u}_k$ are the estimated output and the estimated input from the predictor, respectively. T_s is sampling time. For a fair comparison, the control gains in Cases 1 and 2 were used. the input and output communication delays were 0.5, for all simulation cases. Simulations were performed for one day (24 h), and the control period was set to 1 min.

B. SIMULATION RESULTS

Figure 3 shows the forecast demand and DER power. The power demand is expressed according to the use of home appliances such as TVs, microwaves, washing machines, and air conditioners. As shown in 3(b), there is a power difference between the power supplied by the DER and the demand forecasted by the variable loads.

The imbalanced and desired ESS powers are shown in Fig. 4. From 16 h to 24 h, the highest imbalanced power was observed because several home appliances as interactive demand, were variously operated as shown in Fig. 4(a). Therefore, a larger desired ESS power variation was observed as shown in Fig. 4(b). As the desired ESS power is calculated every minute from (7), it has a smooth continuous signal.

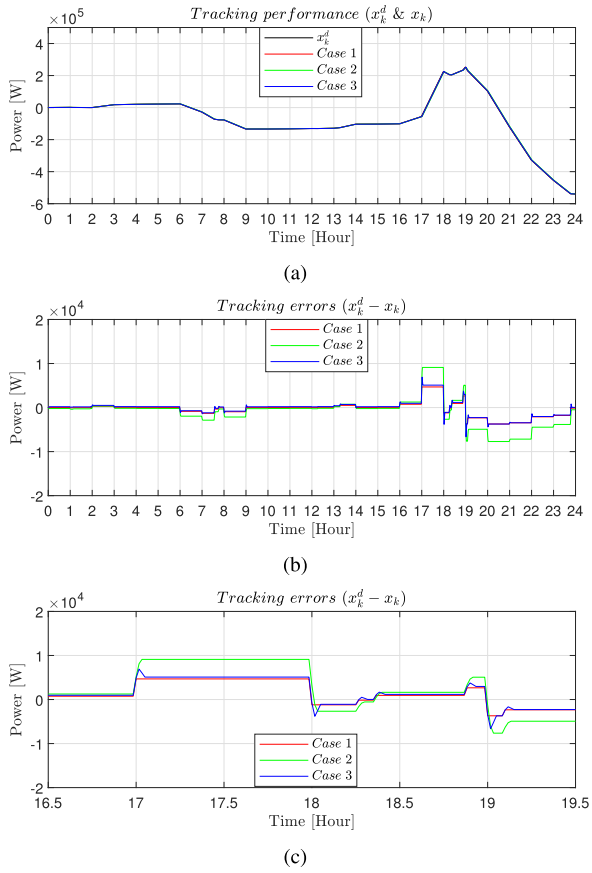

FIGURE 6. Tracking performance and tracking errors (Case 1, 2, and 3): (a) tracking performance, (b) tracking errors, (c) tracking errors (zoomed in x-axis).

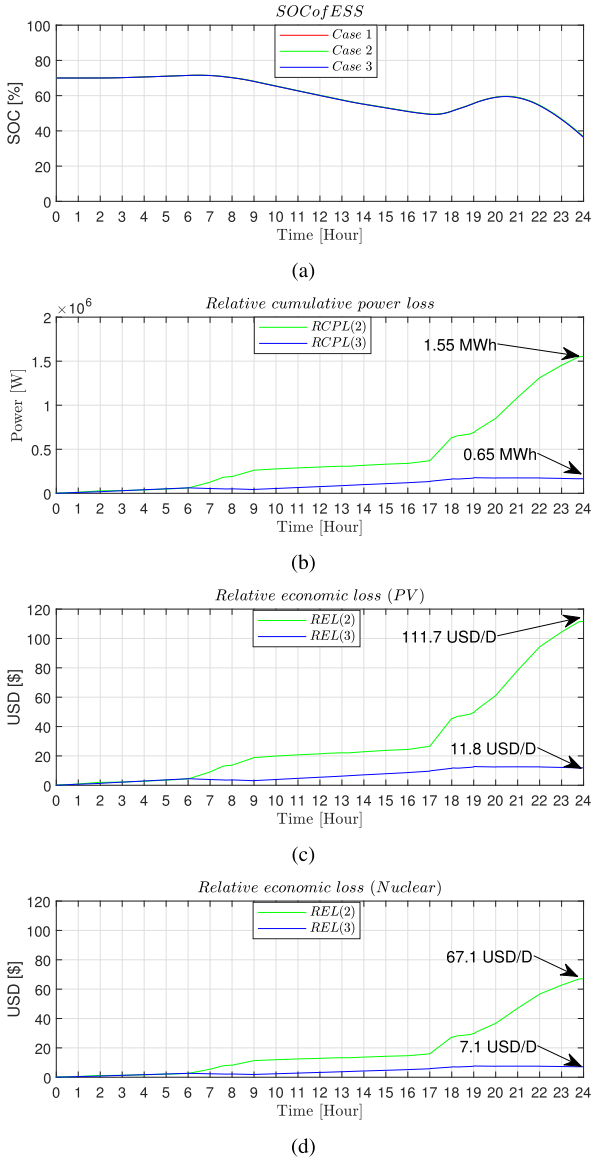

FIGURE 7. SOC and power loss analysis (a) state of charge, (b) relative cumulative power loss, (c) relative economic loss (PV power price), (d) relative economic loss (Nuclear power price).

In contrast, stair signals were observed because the forecasted demand and DER power were measured every 1 h in Figs. 3 and 4(a).

Figure 5 shows the estimation performance and estimation error of the ESS power. The estimated ESS power effectively tracks the actual ESS power using the proposed estimator. At 19 h, the estimation error reached a maximum value of 6.323 kW. Because the actual ESS power was approximately 253.495 kW after 19 h, the percentage error was approximately 2.49 %.

Figure 6 shows the tracking performance and tracking errors of the ESS power. The tracking error in Case 2 was considerably larger than that in Case 1 because of communication delays. However, the tracking error in Case 3 was reduced by designing the proposed controller. This implies that the effect of communication delays was almost eliminated by the proposed controller.

Figure 7 shows the SOC and power loss analysis of the ESS power. In Fig. 7(a), the SOC is proportional to the imbalanced power. For the same initial SOC (70 percentage), after 19 h, the SOC should be decreased to supply power from the ESS to the loads because the demand power suddenly increased. The relative cumulative power loss (RCPL) can be defined to evaluate the power loss depending on the presence of a communication delay as follows:

$$RCPL(N) = \sum_{k=1}^{h} |e_{k(Case\ N)} - e_{k(Case\ 1)}|, \tag{24}$$

where $h = 24 \times 3600 \times F_s$. Here, $F_s = \frac{1}{T_s}$ is the sampling frequency. N is 2 or 3 which is the index of the simulation case for the classical and proposed controls with communication delays. In Fig. 7(b), the RCPL of Case 2 is much larger than that of Case 3 because the classical control has a larger tracking error. To calculate the economic loss, the relative economic loss (REL) was derived using Korea's power generation prices. For a comparison between generation prices, PV generation and nuclear generation have the unit prices of 0.0718 \$/kWh and 0.0432 \$/kWh, respectively,

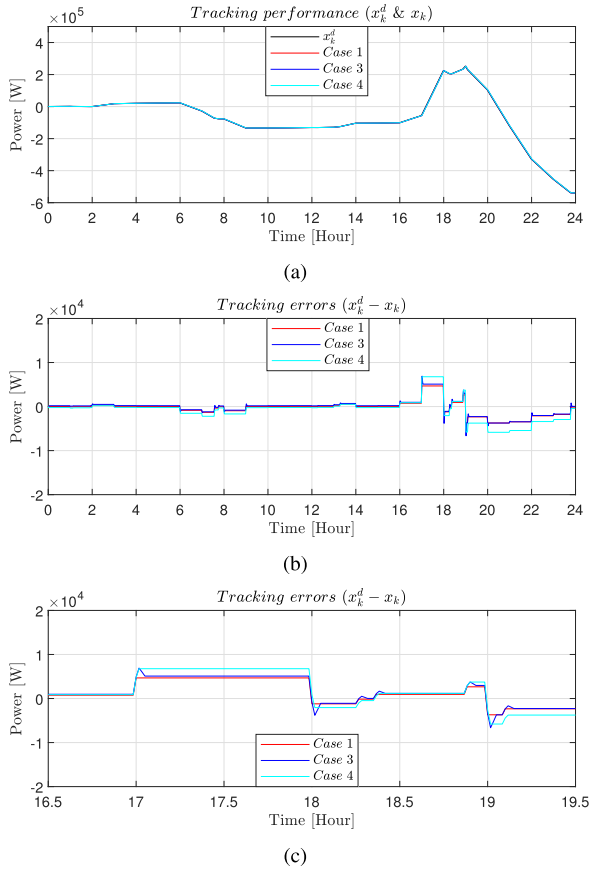

FIGURE 8. Tracking performance and tracking errors (Case 1, 3, and 4): (a) tracking performance, (b) tracking errors, (c) tracking errors (zoomed in x-axis).

as the power generation price (GP).

$$REL(N) = RCPL(N) \times GP. \tag{25}$$

The RELs calculated from (25) are shown in Figs. 7(c) and (d). We observed that the economic loss in Case 2 was larger than that in Case 3 corresponding to the RCPL. Consequently, nuclear generation causes more economic losses than PV generation because of the differences in power generation costs.

Figure 8 shows the tracking performance and tracking errors of the ESS power for Cases 1, 3, and 4. Generally, the predictor accurately estimates the delays in the steady-state region owing to the structural characteristics. Therefore, even if Cases 3 and 4 have similar tracking performances in the steady-state region (slow-varying region), the tracking error in Case 4 is considerably larger than that in Case 3 in the transient region, e.g. from 17 to 20 h. On the other hand, the tracking error of Case 3 is close to that of Case 1 because the proposed controller is robust against communication delays.

Comparisons of the tracking performance and economic evaluation are presented in Tables 1 and 2, respectively. For the tracking performance, the proposed method (Case 3) has the smallest tracking error of approximately 1.2 times,

TABLE 1. Tracking performance analysis.

Performance index	Case 1	Case 2	Case 3	Case 4
Max. tracking error	1	2	3	4
Normalized tracking error	1	2	3	4

TABLE 2. Economic evaluation.

Evaluation index	Predictor (A)	Proposed (B)	Loss rate (A/B)
RCPL	1.55 MWh	0.65 MWh	2.38
REL (PV)	111.7 USD	11.8 USD	9.46
REL (Nuclear)	67.1 USD	7.1 USD	9.45

whereas Cases 2 and 4 have tracking errors of 1.3 times and 1.4 times, respectively, compared with the case with no communication delay (Case 1). For the economic evaluation, the classical predictor exhibits an RCPL and REL of approximately 2.4 and 9.5 times compared with those of the proposed method, respectively.

VI. CONCLUSION

In this paper, we proposed an H_∞ control with input and output communication delays in power systems with both ESSs and DERs. An NG system was defined by considering the dynamics and physical constraints of the load demands, ESSs, and DERs. Subsequently, an ANG system is designed to explain the energy balance between supply and demand. A reference power modulation technique was designed to generate the desired ESS power. Through the application of the proposed reference power modulation technique, the ESS can effectively manage the power status by adjusting the charging power and discharging power. The controller and estimator were developed to improve the tracking performance using information on the ESS power in the presence of communication delays. The tracking and estimation performances of the proposed algorithm were validated through simulations.

The proposed research can be restrictively implemented in situations that require the use of both high power computation processor for real-time implementation and stochastic data for communication delays. This study has limited applicability owing to the limitations of requiring the use of high-end statistical data on communication delays.

A possible future research direction is to demonstrate the closed-loop performance using hardware in the loop simulation for real-time implementation.

APPENDIX

Proof 2: (Proof of Theorem 1) First, the quadratic Lyapunov candidate function can be chosen as follows:

$$V_k = x_k^T P_1 x_k + x_{k-1}^T P_2 x_{k-1} + e_k^T S_1 e_k + e_{k-1}^T S_2 e_{k-1}, \tag{26}$$

where P_1, S_1, P_2 and S_2 are positive definite matrices from the theorem. Using (13), (14), and (26), we obtain

$$\begin{aligned}
&\mathbb{E}\{V_{k+1}|x_k,\cdots,x_0,e_k,\cdots,e_0\}-V_k\\
&=\mathbb{E}\{x_{k+1}^TP_1x_{k+1}+e_{k+1}^TS_1e_{k+1}\}\\
&\quad+x_k^TP_2x_k+e_k^TS_2e_k-x_k^TP_1x_k\\
&\quad-x_{k-1}^TP_2x_{k-1}-e_k^TS_1e_k-e_{k-1}^TS_2e_{k-1}\\
&=\{[\Phi+(1-\bar\beta)\Gamma K]x_k-(1-\bar\beta)\Gamma Ke_k+\bar\beta\Gamma Kx_{k-1}\\
&\quad-\bar\beta\Gamma Ke_{k-1}\}^TP_1\{[\Phi+(1-\bar\beta)\Gamma K]x_k-(1-\bar\beta)\Gamma Ke_k\\
&\quad+\bar\beta\Gamma Kx_{k-1}-\bar\beta\Gamma Ke_{k-1}\}\\
&\quad+\{[\Phi-(1-\bar\alpha)LC]e_k-\bar\alpha LCe_{k-1}\}^TS_1\\
&\quad\times\{[\Phi-(1-\bar\alpha)LC]e_k-\bar\alpha LCe_{k-1}\}\\
&\quad+(1-\bar\beta)\bar\beta[\Gamma K]^T[x_k-e_k-x_{k-1}+e_{k-1}]^TP_1\Gamma K\\
&\quad\times[x_k-e_k-x_{k-1}+e_{k-1}]\\
&\quad+(1-\bar\alpha)\bar\alpha[LCx_k-LCx_{k-1}]^TS_1[LCx_k-LCx_{k-1}]^T\\
&\quad+x_k^TP_2x_k+e_k^TS_2e_k+x_k^TP_1x_k-x_{k-1}^TP_2x_{k-1}\\
&\quad-e_k^TS_1e_k-e_{k-1}^TS_2e_{k-1}\\
&=\chi_k^T\Xi\chi_k
\end{aligned}\tag{27}$$

where Ξ can be defined in (28) with the conditions of $\mathbb{E}\{(\alpha-\bar\alpha)^2\}=(1-\bar\alpha)\bar\alpha$ and $\mathbb{E}\{(\beta-\bar\beta)^2\}=(1-\bar\beta)\bar\beta$.

$$\begin{aligned}
\Xi&=\Xi_1^T\Xi_2\Xi_1+\Xi_3\\
\Xi_1&=\begin{bmatrix}\Phi+(1-\bar\beta)\Gamma K & -(1-\bar\beta)\Gamma K & \bar\beta\Gamma K & -\bar\beta\Gamma K\\ 0 & \Phi+(1-\bar\alpha)LC & 0 & -\bar\alpha LC\\ \Gamma K & -\Gamma K & -\Gamma K & \Gamma K\\ LC & 0 & -LC & 0\end{bmatrix}\\
\Xi_2&=\begin{bmatrix}P_1 & 0 & 0 & 0\\ 0 & S_1 & 0 & 0\\ 0 & 0 & (1-\bar\beta)\bar\beta P_1 & 0\\ 0 & 0 & 0 & (1-\bar\alpha)\bar\alpha S_1\end{bmatrix}\\
\Xi_3&=\begin{bmatrix}P_2-P_1 & 0 & 0 & 0\\ 0 & S_2-S_1 & 0 & 0\\ 0 & 0 & -P_2 & 0\\ 0 & 0 & 0 & -S_2\end{bmatrix}
\end{aligned}\tag{28}$$

As P_1 and S_1 in (28) are positive definite, this implies $\Xi<0$ by the definition of the Schur complement. For the stability analysis of the closed-loop system in (13), we obtain the following statement:

$$\begin{aligned}
&\mathbb{E}\{V_{k+1}|x_k,\cdots,x_0,e_k,\cdots,e_0\}-V_k\\
&\quad=\chi_k^T\Xi\chi_k\le-\lambda_{min}(-\Xi)\chi_k^T\chi_k<q\chi_k^T\chi_k
\end{aligned}\tag{29}$$

where $0<q<min\{-\lambda_{min}(\Xi),\sigma\}$. σ is the maximum eigenvalue of P_1, S_1, P_2, and S_2. Therefore, based on Definition 1 and Lemma 1, the origin of the closed-loop system in (13) is exponentially stable with (30). This completes the proof of the theorem.

$$M=\begin{bmatrix}M_{11} & M_{12}\\ M_{21} & M_{22}\end{bmatrix}$$

$$\begin{aligned}
M_{11}&=\begin{bmatrix}P_2-P_1 & * & * & *\\ 0 & S_2-S_1 & * & *\\ 0 & 0 & -P_2 & *\\ 0 & 0 & 0 & -S_2\end{bmatrix}\\
M_{12}&=\begin{bmatrix}*&*&*&*\\ *&*&*&*\\ *&*&*&*\\ *&*&*&*\end{bmatrix}\\
M_{21}&=\begin{bmatrix}\Phi+(1-\bar\beta)\Gamma K & -(1-\bar\beta)\Gamma K & \bar\beta\Gamma K & -\bar\beta\Gamma K\\ 0 & \Phi+(1-\bar\alpha)LC & 0 & -\bar\alpha LC\\ \Gamma K & \Gamma K & \Gamma K & \Gamma K\\ LC & 0 & -LC & 0\end{bmatrix}\\
M_{22}&=\begin{bmatrix}-P_1^{-1} & * & * & *\\ 0 & -S_1^{-1} & * & *\\ 0 & 0 & -\kappa_2^{-2}P_1^{-1} & *\\ 0 & 0 & 0 & -\kappa_1^{-2}S_1^{-1}\end{bmatrix}
\end{aligned}\tag{30}$$

$$Q=\begin{bmatrix}Q_{11} & Q_{12}\\ Q_{21} & Q_{22}\end{bmatrix}<0$$

$$\begin{aligned}
Q_{11}&=\begin{bmatrix}P_2-P_1 & * & * & * & *\\ 0 & S_2-S_1 & * & * & *\\ 0 & 0 & -P_2 & * & *\\ 0 & 0 & 0 & -S_2 & *\\ * & * & * & * & -\gamma^2I\end{bmatrix}\\
Q_{12}&=\begin{bmatrix}*&*&*&*&*\\ *&*&*&*&*\\ *&*&*&*&*\\ *&*&*&*&*\\ *&*&*&*&*\end{bmatrix}\\
Q_{21}&=\begin{bmatrix}\Phi+\Gamma K & -(1-\bar\beta)\Gamma K & \bar\beta\Gamma K & -\bar\beta\Gamma K & \Gamma_w\\ -\bar\beta\Gamma K & & & & \\ 0 & \Phi-LC & 0 & -\bar\alpha LC & (1-\bar\alpha)\\ & -\bar\alpha LC & & & LC_w\Gamma_w\\ \Gamma K & -\Gamma K & \Gamma K & -\Gamma K & 0\\ LC & 0 & -LC & 0 & 0\\ D & 0 & 0 & 0 & F_w\end{bmatrix}\\
Q_{22}&=\begin{bmatrix}-P_1^{-1} & * & * & * & *\\ 0 & -S_1^{-1} & * & * & *\\ 0 & 0 & -\kappa_2^{-2}P_1^{-1} & * & *\\ 0 & 0 & 0 & -\kappa_1^{-2}S_1^{-1} & *\\ 0 & 0 & 0 & 0 & -I\end{bmatrix}
\end{aligned}\tag{31}$$

$$W=\begin{bmatrix}W_{11} & W_{12}\\ W_{21} & W_{22}\end{bmatrix}<0$$

$$\begin{aligned}
W_{11}&=\begin{bmatrix}P_2-P_1 & * & * & * & *\\ 0 & S_2-S_1 & * & * & *\\ 0 & 0 & -P_2 & * & *\\ 0 & 0 & 0 & -S_2 & *\\ * & * & * & * & -\gamma^2I\end{bmatrix}\\
W_{12}&=\begin{bmatrix}*&*&*&*&*\\ *&*&*&*&*\\ *&*&*&*&*\\ *&*&*&*&*\\ *&*&*&*&*\end{bmatrix}
\end{aligned}$$

$$W_{21} = \begin{bmatrix} P_1\Phi + \\ (1-\bar{\beta}) \\ \Gamma M \end{bmatrix} \begin{matrix} -(1-\bar{\beta}) \\ \Gamma M \end{matrix} \quad \bar{\beta}\Gamma K \quad -\bar{\beta}\Gamma K \quad P_1\Gamma_w$$
$$\begin{matrix} 0 \end{matrix} \quad \begin{matrix} S_1\Phi \\ (1-\bar{\alpha}) \\ NC \end{matrix} \quad \begin{matrix} 0 \end{matrix} \quad \begin{matrix} -\bar{\alpha}NC \end{matrix} \quad \begin{matrix} S_1 \\ (1-\bar{\alpha}) \\ NC_w\Gamma_w \end{matrix}$$
$$\begin{matrix} \kappa_2\Gamma M \\ \kappa_1 NC \\ D \end{matrix} \quad \begin{matrix} -\kappa_2\Gamma M \\ 0 \\ 0 \end{matrix} \quad \begin{matrix} -\kappa_2\Gamma M \\ -\kappa_1 NC \\ 0 \end{matrix} \quad \begin{matrix} \kappa_2\Gamma M \\ 0 \\ 0 \end{matrix} \quad \begin{matrix} 0 \\ 0 \\ F_w \end{matrix}$$

$$W_{22} = \begin{bmatrix} -P_1^{-1} & * & * & * & * \\ 0 & -S_1^{-1} & * & * & * \\ 0 & 0 & -P_1^{-1} & * & * \\ 0 & 0 & 0 & -S_1^{-1} & * \\ 0 & 0 & 0 & 0 & -I \end{bmatrix} \tag{32}$$

■

Proof 3: (Proof of Theorem 2) The objective function with the H_∞ constraint is defined as follows:

$$\mathbb{E}\{V_{k+1}\} - \mathbb{E}\{V_k\} + \mathbb{E}\{z_k^T z_k\} - \gamma^2 \mathbb{E}\{w_k^T w_k\} < 0 \tag{33}$$

where V_k represents the quadratic Lyapunov function in (26). The equivalent form of (33) can be represented as

$$\mathbb{E}\left\{ \begin{bmatrix} \chi_k \\ w_k \end{bmatrix}^T \begin{bmatrix} \Xi + D_T^T D_T & \Gamma_3^T P_1 \Gamma_w + \Gamma_4^T S_1 \Gamma_w \\ \Gamma_w^T P_1 \Gamma_3 + \Gamma_w^T S_1 \Gamma_4 & \Gamma_w^T (P_1 + S_1)\Gamma_w \\ & + F_w^T F_w - \gamma^2 I \end{bmatrix} \begin{bmatrix} \chi_k \\ w_k \end{bmatrix} \right\} < 0 \tag{34}$$

where Ξ is given by (30), and $\Gamma_3 = \begin{bmatrix} \Phi + (1-\bar{\beta})\Gamma K \\ -(1-\bar{\beta})\Gamma K \\ \bar{\beta}\Gamma K \\ -\bar{\beta}\Gamma K \end{bmatrix}^T$,

$\Gamma_4 = \begin{bmatrix} 0 \\ \Phi - (1-\bar{\alpha})LC \\ 0 \\ \bar{\alpha}LC \end{bmatrix}$, $D^T = \begin{bmatrix} D \\ 0 \\ 0 \\ 0 \end{bmatrix}^T$. From the definition of the Schur complement, the matrix inequality in (34) holds. Definition 2 yields the H_∞ performance of the closed-loop system. In addition, from the theorem and $w_k = 0$, we have the inequality $\Xi + D_T^T D_T < 0$. Then this implies $\Xi < 0$. According to Theorem 1, the origin of a closed-loop system is exponentially stable. This completes the proof. ■

REFERENCES

[1] M. F. Zia, E. Elbouchikhi, and M. Benbouzid, "Microgrids energy management systems: A critical review on methods, solutions, and prospects," *Appl. Energy*, vol. 222, pp. 1033–1055, Jul. 2018.

[2] Y. Gui, R. Han, J. M. Guerrero, J. C. Vasquez, B. Wei, and W. Kim, "Large-signal stability improvement of DC–DC converters in DC microgrid," *IEEE Trans. Energy Convers.*, vol. 36, no. 3, pp. 2534–2544, Sep. 2021.

[3] Y. Du, J. Wu, S. Li, C. Long, and S. Onori, "Coordinated energy dispatch of autonomous microgrids with distributed MPC optimization," *IEEE Trans. Ind. Informat.*, vol. 15, no. 9, pp. 5289–5298, Sep. 2019.

[4] D. Burmester, R. Rayudu, W. Seah, and D. Akinyele, "A review of nanogrid topologies and technologies," *Renew. Sustain. Energy Rev.*, vol. 67, pp. 760–775, Jan. 2017.

[5] S. A. G. K. Abadi, J. Choi, and A. Bidram, "A method for charging electric vehicles with battery-supercapacitor hybrid energy storage systems to improve voltage quality and battery lifetime in islanded building-level DC microgrids," *IEEE Trans. Sustain. Energy*, vol. 14, no. 3, pp. 1–14, Oct. 2023.

[6] S. Javaid, Y. Kurose, T. Kato, and T. Matsuyama, "Cooperative distributed control implementation of the power flow coloring over a nano-grid with fluctuating power loads," *IEEE Trans. Smart Grid*, vol. 8, no. 1, pp. 342–352, Jan. 2017.

[7] J. Leitão, P. Gil, B. Ribeiro, and A. Cardoso, "A survey on home energy management," *IEEE Access*, vol. 8, pp. 5699–5722, 2020.

[8] X. Wang, X. Mao, and H. Khodaei, "A multi-objective home energy management system based on Internet of Things and optimization algorithms," *J. Building Eng.*, vol. 33, Jan. 2021, Art. no. 101603.

[9] R. Wang, Q. Sun, J. Hu, S. Jiang, H. Huang, and Y. Gui, "Disturbance observer based generalized wind/solar/battery consistent control strategy for AC microgrids," *Int. Trans. Electr. Energy Syst.*, vol. 31, no. 10, Oct. 2021, Art. no. e12539.

[10] C. Ju, P. Wang, L. Goel, and Y. Xu, "A two-layer energy management system for microgrids with hybrid energy storage considering degradation costs," *IEEE Trans. Smart Grid*, vol. 9, no. 6, pp. 6047–6057, Nov. 2018.

[11] J. Yim, S. You, F. Blaabjerg, Y. Lee, Y. Gui, and W. Kim, "Energy management systems for forecasted demand error compensation using hybrid energy storage system in nanogrid," *Renew. Energy*, vol. 221, Feb. 2024, Art. no. 119744.

[12] M. Beaudin and H. Zareipour, "Home energy management systems: A review of modelling and complexity," *Renew. Sustain. Energy Rev.*, vol. 45, pp. 318–335, May 2015.

[13] R. E. Edwards, J. New, and L. E. Parker, "Predicting future hourly residential electrical consumption: A machine learning case study," *Energy Buildings*, vol. 49, pp. 591–603, Jun. 2012.

[14] Y. Ding, Z. Wang, S. Liu, and X. Wang, "Energy management strategy of PV grid-connected household nano-grid system," in *Proc. IEEE Power Energy Soc. Gen. Meeting (PESGM)*, Aug. 2019, pp. 1–5.

[15] F. Yang, Z. Wang, Y. S. Hung, and M. Gani, "H_∞ control for networked systems with random communication delays," *IEEE Trans. Automat. Contr.*, vol. 51, no. 3, pp. 511–518, Jul. 2006.

[16] M. Jin, S. H. Kang, P. H. Chang, and J. Lee, "Robust control of robot manipulators using inclusive and enhanced time delay control," *IEEE/ASME Trans. Mechatronics*, vol. 22, no. 5, pp. 2141–2152, Oct. 2017.

[17] Y. Zuo, Y. Wang, X. Liu, S. X. Yang, L. Huang, X. Wu, and Z. Wang, "Neural network robust H_∞ tracking control strategy for robot manipulators," *Appl. Math. Model.*, vol. 34, pp. 1823–1838, Aug. 2010.

[18] Y. Lee, J. Moon, W. Kim, C. C. Chung, and M. Tomizuka, "H_∞ control using linear parameter varying approach for motion control systems under communication delays: Application to PMSM," *J. Electr. Eng. Technol.*, vol. 15, no. 4, pp. 1797–1809, Jul. 2020.

[19] J. Doyle, K. Glover, P. Khargonekar, and B. Francis, "State-space solutions to standard H_2 and H_∞ control problems," *IEEE Trans. Autom. Control*, vol. 34, no. 8, pp. 831–847, Aug. 1989.

[20] (2019). *Korea Power Exchange, 2019 Residential Appliance Penetration Survey Report*. Accessed: Apr. 22, 2022. [Online]. Available: https://www.data.go.kr/data/15065241/fileData.do

[21] (2022). *Korea Power Exchange, Kepco_seoul Solar Power Generation*. Accessed: Jul. 29, 2022. [Online]. Available: https://www.data.go.kr/data/15065737/fileData.do

[22] A. Bertino, P. Naseradinmousavi, and M. Krstic, "Delay-adaptive control of a 7-DOF robot manipulator: Design and experiments," *IEEE Trans. Control Syst. Technol.*, vol. 30, no. 6, pp. 2506–2521, Nov. 2022.

[23] N. Espitia and W. Perruquetti, "Predictor-feedback prescribed-time stabilization of LTI systems with input delay," *IEEE Trans. Autom. Control*, vol. 67, no. 6, pp. 2784–2799, Jun. 2022.

[24] X. Xu, L. Liu, M. Krstic, and G. Feng, "Stability analysis and predictor feedback control for systems with unbounded delays," *Automatica*, vol. 135, Jan. 2022, Art. no. 109958.

YOUNGWOO LEE (Member, IEEE) received the B.S. degree in electrical engineering from Chungbuk National University, Cheongju-si, South Korea, in 2010, and the Ph.D. degree in electrical engineering from Hanyang University, Seoul, South Korea, in 2017. From 2017 to 2018, he was a Research Scientist with Ulsan National Institute of Science Technology and a Postdoctoral Researcher with the Department of Mechanical Engineering, University of California at Berkeley, CA, USA. From 2018 to 2019, he was with the Memory Division, Samsung Electronics Ltd., South Korea. From 2019 to 2020, he was an Assistant Professor with the Department of Electronics Engineering, Pai Chai University, Daejeon, South Korea. In 2020, he joined as a Faculty Member with Chonnam National University, Gwangju, South Korea. He is currently an Associate Professor with the Division of Electrical Engineering, Hanyang University, ERICA Campus, Ansan, South Korea. His research interests include power system optimization, electric machine control, and nonlinear and optimal controller design.

YONGHAO GUI (Senior Member, IEEE) received the B.S. degree in automation from Northeastern University, Shenyang, China, in 2009, and the M.S. and Ph.D. degrees in electrical engineering from Hanyang University, Seoul, South Korea, in 2012 and 2017, respectively.

From 2017 to 2022, he was with Aalborg University, Aalborg, Denmark, as a Postdoctoral Researcher and then an Assistant Professor. In 2022, he was with Vestas, Denmark. Currently, he is with the Oak Ridge National Laboratory, USA. His research interests include control of power electronics in power systems, renewable energy integration, and cyber-physical systems.

Dr. Gui was a recipient of the Best Paper in IEEE TRANSACTIONS ON ENERGY CONVERSIONS, in 2021; the IEEE Power and Energy Society General Meeting Best Conference Paper Award, in 2019, and the Best Paper Award in IEEEComputational Intelligence Society Conference, in 2023. He served as an Editor for IEEE TRANSACTIONS ON SUSTAINABLE ENERGY, IEEE TRANSACTIONS ON ENERGY CONVERSION, and IEEE POWER ENGINEERING LETTERS; and an Associate Editor for IEEE TRANSACTIONS ON INDUSTRIAL ELECTRONICS and IEEE ACCESS.

WONHEE KIM (Member, IEEE) received the B.S. and M.S. degrees in electrical and computer engineering and the Ph.D. degree in electrical engineering from Hanyang University, Seoul, South Korea, in 2003, 2005, and 2012, respectively. From 2005 to 2007, he was with Samsung Electronics Company, Suwon, South Korea. In 2012, he was with the Power and Industrial Systems Research and Development Center, Hyosung Corporation, Seoul. In 2013, he was a Postdoctoral Researcher with the Institute of Nano Science and Technology, Hanyang University, and a Visiting Scholar with the Department of Mechanical Engineering, University of California at Berkeley, CA, USA. From 2014 to 2016, he was with the Department of Electrical Engineering, Dong-A University, Busan, South Korea. He is currently a Professor with the School of Energy Systems Engineering, Chung-Ang University, Seoul. His current research interests include nonlinear control and nonlinear observers and their industrial applications.